SIMULATION OF THE DIFFUSION PROCESS OF NaCl AND KCl IN OLIVE PULP USING THE FINITE ELEMENT METHOD

Marco A. J. Clemente[a], **Heloisa H. P. Silva**[a], **Nathan F. Silva**[a], **Julia W. Campos**[a], **Eduardo G. de Sousa**[a], **Hágata C. Silva**[a], **Ana C. G. Mantovani**[b], [iD], **Karina B. Angilelli**[a] and **Dionisio Borsato**[a],*,[iD]

[a]Departamento de Química, Universidade Estadual de Londrina, 86057-970 Londrina – PR, Brasil
[b]Centro Universitário Ingá, 87035-510 Maringá – PR, Brasil

The simultaneous diffusion of inorganic components in the olive pulp in wet brine was modeled based on Fick's generalized 2nd Law and simulated using the finite element method. The main and crossed diffusion coefficients, the film coefficient and the Biot number were determined, with the application of the simplex optimization method, through the minimization of the percentage errors. The errors between the simulated and experimental data were 5.35% for NaCl and 4.77% for KCl and the adjusted main diffusion coefficients were 0.4358×10^{-12} m^2 s^{-1} for NaCl and 0.5408×10^{-12} m^2 s^{-1} for KCl. The system developed to simulate diffusion allows the control and modulation of the salts content that diffuses through the olive pulp.

Keywords: Fick's law; simplex optimization; multicomponent diffusion.

INTRODUCTION

The olive is the fruit of the olive tree (*Olea Europea*) and is one of the most consumed fruits in Mediterranean countries, with Spain, Portugal, and Greece being the largest producers. It is composed of elements such as potassium, magnesium, calcium, and sodium and has a high concentration of vitamin E and phenolic compounds, including oleuropein, responsible for the fresh fruit bitterness, tyrosol, and hydroxytyrosol. As fresh olives can be easily spoiled due to high water activity until processing, they must undergo treatment in brines or be used for oil production.[1-6]

In brine treatment, the main component is sodium chloride (NaCl) which is responsible for the preservative, flavoring, and delaying the action of unwanted microorganisms' development. Despite this, NaCl excess in the diet can cause cardiovascular and kidney diseases.[7,8] The consumption of foods with low sodium content has been a concern of the most attentive consumers, preventive medicine and the food industry.[9]

To reduce the negative effects of high sodium chloride consumption, some researchers recommend the partial replacement of NaCl with other salts, such as calcium and potassium chloride in amounts that do not cause changes in its sensory properties.[7-11]

In the conservation process, the natural olives, harvested at full maturity or a little earlier, are washed to remove surface residues and immersed in brine containing 6 to 10% (m/v) of sodium chloride, which is responsible for reducing the taste of oleuropein. This method consists of slowly diffusing the salt through the olive pulp until equilibrium.[8,12,13]

Several models of water loss and solute gain are based on the assumption that mass transfer can be described by the Fick diffusion equation (2nd law) in a non-stationary regime. A wide variety of solutions to Fick's 2nd law is presented by Crank.[14]

Diffusion theories are well established and new applications have enabled more realistic modeling of mass transfer in food processes.[9,15,16]

When a fluid is in contact with a solid surface, a film forms on the surface. If there is a mass transfer between the surface and the fluid, the current has to cross the stationary layer that acts as a resistance.[17,18] Therefore, this diffusion process can be composed of a series of mass transfer mechanisms, being necessary to consider the resistances to mass diffusivity, both, internal and external. Such hypotheses, commonly used, are quantified by the mass Biot number.[17] According to some authors, the higher the Biot number, the lower the influence of external resistance on the diffusion mechanism. If the value of the mass Biot number is greater than 200, the relative error in determining the diffusion coefficient, due to neglecting the external resistance, is less than 1. Therefore, a high Biot number indicates that the internal resistance is limiting and as this value decreases, the external resistance increases, evidencing an interference of the closest layer of solution in the solid surface contours.[17,19]

With the availability of high-speed processors, researchers and designers have the opportunity to simulate industrial processes in their closest way to reality. A numerical technique currently used to solve problems that are described by partial differential equations is the finite element method (FEM). The main advantages of this method are that the spatial variation of material properties can be easily manipulated, irregular regions can be modeled with great precision, the method is the most suitable for non-linear problems, the dimensions of the elements can be easily changed, spatial interpolation is much more realistic and problems with the most diverse boundary conditions can be efficiently worked out.[20]

Several authors have investigated heat and/or mass transfer by applying the finite element formulation.[9,15,16,21-23] The finite element method is a set of efficient techniques that obtain numerical solutions to differential equations, which can be applied in the most varied fields of sciences, particularly in engineering, physics and chemistry problems.[11,24,25] The method is general in terms of geometry and material properties. More complex and irregular bodies composed of different materials are conveniently represented since irregular shapes can be approximated because each element can be different.[24]

System optimization is an adjusting process for the factors that influence them in an attempt to produce the best result. The optimization processes are divided into steps, characterized by decisions about the function to be observed, determining the factors that significantly influence the response and the actual optimization of the selected variables.[9] Over the years, several optimization methods

have been developed. A proposal known as simplex was presented by Spendley *et al.*[26] The simplex is a regular figure that moves over a surface to avoid regions of unsatisfactory response. The method is a recurrent procedure, which tends to bring the simplex to an optimal value by reflecting specific points. Once in the vicinity of the optimum, the simplex can undergo contraction to determine a more precise position.[9]

The objective of this work was to study the diffusion of inorganic chemical species during the olive brining process and to determine the diffusion coefficients, Biot number and the skin coefficient simulating the process through the finite element method associated with simplex optimization.

EXPERIMENTAL

Olives

Olives of the Arbequina variety were used, produced in the city of Ventania - PR, Brazil - 24 06' 58" S, 50 11' 31" W - whose average dimensions, obtained with a digital pachymeter are shown in Figure 1.

Brine Preparation and Sampling

12 L of brine with 10% (w/v) salt, containing 30% potassium chloride and 70% sodium chloride were used. The olive samples were completely immersed in the brine, without previous treatment, being collected at 0, 6, 12, 14, 15, 17, 18, 22, 25, 33, 39, 45, 51, 57, and 60 hours. Each sample consisted of a set of pulps from three olives.

Centesimal Composition

The quantification of the moisture content in fresh samples was carried out by drying the olives in an oven at 105 °C until obtained a constant weight. For the protein content, the Kjeldahl Method was used, considering a conversion factor of the total nitrogen content to the protein percentage of 6.25%. The ash was determined by incineration in a muffle furnace at 550 °C. The lipid content was analyzed gravimetrically after extraction with petroleum ether using the Soxhlet extractor device. The total carbohydrate content in the olive pulp was determined by the percentage difference between the total mass and the sum of the other components: proteins, lipids, ash and moisture. The physicochemical characteristics of the olive pulp were determined in triplicate.

Determination of Sodium and Potassium Concentrations

The concentrations of NaCl and KCl in olive pulp samples were determined according to the methodology described by Bordin *et al.*,[9] with modifications, using the Micronal photometer, model B-462, with an air pressure of 0.8 kgf cm^{-2} and air pump pressure of 1.5 kgf cm^{-2} using butane gas.

Three-Dimensional Modeling

The modeling was performed using the finite element method considering three-dimensional mass transfer, Fick's second law equations[18] and Onsager's equations[27] according to equation 1.

$$\frac{\partial C_1}{\partial t} = D_{11}\nabla^2 C_1 + D_{12}\nabla^2 C_2 \text{ and } \frac{\partial C_2}{\partial t} = D_{21}\nabla^2 C_1 + D_{22}\nabla^2 C_2 \qquad (1)$$

where D_{11}, D_{22} and D_{12}, D_{21} are the main and cross diffusion coefficients, respectively and $\nabla^2(.) = \nabla.\nabla(.)$ is the Laplacian operator.

The diffusion coefficient was considered constant, regardless of the position and immersion time in the brine. The solute diffusion occurred under isothermal conditions (20 °C) and the contraction of the olive samples during salting was considered negligible. To determine the diffusion coefficients and evaluate the influence of the film formed on the olive surface, the Cauchy boundary condition was considered and described in mathematical terms by equations 2 and 3, respectively. The initial concentrations of NaCl and KCl in olive are represented by $C_{1,0}$ and $C_{2,0}$.[28]

$$C_1(x, y, z, 0) = C_{1,0} \text{ and } C_2(x, y, z, 0) = C_{2,0} \text{ } x,y,z \in \Omega \qquad (2)$$

$$\frac{\partial C_1(R,t)}{\partial n} = \frac{h_m}{\lambda_m}[C_1 - C_{1,s}] \text{ and } \frac{\partial C_2(\pm R,t)}{\partial n} = \frac{h_m}{\lambda_m}[C_2 - C_{2,s}] \text{ } x,y,z \in \partial\Omega, \text{ } t > 0 \quad (3)$$

where h_m (m s^{-1}) is the mass transfer coefficient, λ_m (m^2 s^{-1}) the mass conductivity, $\partial\Omega$ the domain, $\partial/\partial\eta$ the operator of the normal derivative. The concentrations of the solutes present in the brine in direct contact with the olive are represented by $C_{1,s}$ and $C_{2,s}$. The coefficients h_m and λ_m are associated with the Biot number according to equation 4, which provides the ratio of the internal and external resistance of the mass transfer.

$$Bi = \frac{h_m.R_i}{\lambda_m}; i = 1,2,3 \qquad (4)$$

where R_i is the characteristic dimension.

The finite element formulation followed the procedures established by Cremasco *et al.*[18] The flux was established only in the olive pulp whose domain, orientation and extra fine regular tetrahedral mesh, with 127,044 elements, are represented in Figure 1.
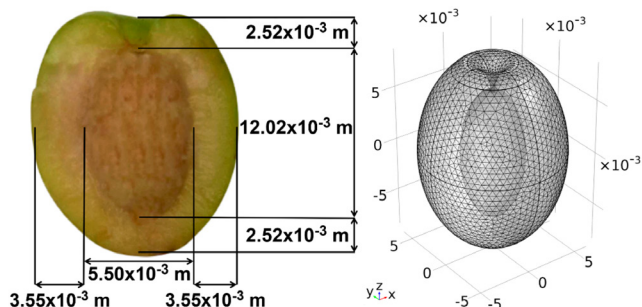

Figure 1. *Average dimensions of the olives collected, the orientation and mesh generated by the finite element method (FEM)*

Statistical Test

The optimization was performed by minimizing the percentage error according to equation 5.[29]

$$\text{Error \%} = 100 \sum_{i=1}^{N} \left[\frac{|\overline{C}_{calc} - \overline{C}_{exp}|}{\overline{C}_{exp}} \right] \frac{1}{N} \qquad (5)$$

being $\overline{C}_{exp}$ the average experimental concentration, $\overline{C}_{calc}$ the concentration simulated by the numerical solution and N the number of observations considered.

Diffusion Coefficients and h_m/λ_m

The adjustment of the main and cross coefficients and the h_m/λ_m ratio was performed by applying the optimization by the super modified simplex method coupled to the desirability function (DF),

using an algorithm originally developed by Harrington[30] and later improved by Derringer and Suich.[31]

Several coefficient associations were generated by the COMSOL[32] software via the finite element method and compared using the optimization algorithm. With these new simulated concentrations, they were compared with the experimental ones, providing new percentage errors calculated by equation 5. By minimizing the errors, this process was repeated until the stability of the values found for the percentage errors and main, crossed coefficients, h_m/λ_m; where h_m (m s^{-1}) is the mass transfer coefficient of the solute in the film formed around the olive and λ_m (m^2 s^{-1}) is the mass conductivity.[9,29,33]

Computer Program and Processing

An Intel® Core™ i7-4790 CPU© 3.60 GHz computer was used, with 32 GB RAM with 250 GB HDD. The diffusion process was simulated by the COMSOL[32] Multiphysics® software version 5.2 (COMSOL, Inc., Burlington, MA) using the finite element method.

RESULTS AND DISCUSSION

Samples of *in natura* olives, before starting the salting process, were submitted to the centesimal composition assay and the values corresponding to the moisture, lipid, carbohydrate, protein, ash, sodium chloride and potassium chloride contents of the olive pulp are shown in Table 1. The results of the centesimal composition assay except for the oil and carbohydrate content, are similar to the values presented by Öngen *et al.*[34] cited by Colak & Hepbasli,[4] that is, 14.67% and 3.32% respectively. Water is the major component in the composition of the olive, with an average value of 69.63%. According to Malheiro *et al.*[35] the ash content (1.31%) does not vary considerably with the cultivar.

It can be seen in Table 1 that the concentration of sodium chloride is higher than that of potassium chloride. Saúde,[36] studying the production of olives in brines with low sodium chloride content, using the Maçanilha cultivar, showed that the sodium content, in fresh samples, is higher than the potassium content. Ünal & Nergiz[37] analyzed the composition of Memecik olives and showed that the potassium content was higher than the sodium content. We can see that the sodium and potassium content of fresh olives depends on the variety and geographical origin. In Table 1, the sodium and potassium chloride contents are already included in the ash content.

Table 1. Centesimal composition of olive pulps before diffusion by immersion

Composition	g 100 g^{-1}
Moisture	69.63
Ash	1.31
Lipids	5.16
Protein	1.42
Carbohydrate	22.48
NaCl	0.029
KCl	0.022

According to Fernándes *et al.*,[38] Gómez *et al.*,[39] Hurtado *et al.*[40] and Cardoso *et al.*[41] the production of preserved olives is delayed due to the slow diffusion of the compounds through the skin to the outside and because the oleuropein solubilization in the brine is slow. The equilibrium is reached between 8 to 12 months when all the fermentable substrates, mostly sugars, are exhausted.

To simulate the diffusion process of sodium and potassium chloride, the olive samples were immersed in brine for 60 hours.

During the salting period, three samples of olives were collected at each sampling time. The dimensions of each sample were determined, and the pulp was removed, weighed and placed in porcelain crucibles to determine the moisture and the sodium and potassium chloride content. Figure 1 shows the average dimensions of width, height and pulp as well as the mesh used in the simulation procedure by the FEM. At the beginning and end of the salting period, the concentrations of NaCl and KCl in the brine were determined. The final concentrations did not show a significant difference at a level of 5% when compared to the beginning of the salting process, since to keep the concentration of salts in the brine constant, the ratio between its volume and the volume occupied by the olives was 50:1.

With the data of the salts' concentrations in the olive pulp at the established sampling times, during the salting process by immersion, it was possible to adjust the main and cross-diffusion coefficients and the ratio between the film coefficients and mass conductivity (h_m/λ_m) using the finite element method and the optimization applying the super modified simplex method. As the simplex method is recursive and with constraints, to avoid an optimization with many steps, the lower and upper limits of each parameter, described in Table 2, were established based on preliminary tests.[9,11]

Table 2. Lower and upper limit of the main, cross and h_m/λ_m diffusion coefficients used in simplex optimization

	Lower Limit	Upper Limit
NaCl main coefficient (m^2 s^{-1})	0.2200×10^{-12}	0.5000×10^{-12}
KCl main coefficient (m^2 s^{-1})	0.4500×10^{-12}	0.7000×10^{-12}
NaCl cross coefficient (m^2 s^{-1})	0.0250×10^{-12}	0.0450×10^{-12}
KCl cross coefficient (m^2 s^{-1})	0.0150×10^{-12}	0.0500×10^{-12}
h_m/λ_m (m^{-1})	19,718.3100	33,802.8200

(h_m): mass transfer coefficient. (λ_m): diffusivity coefficient.

In the optimization of the main and cross-diffusion coefficients and the h_m/λ_m ratio, Equation 5 was applied to minimize and stabilize the values of the percentage errors between the simulated and experimental concentrations using the joint optimization represented by the desirability function (DF).[42]

This procedure was carried out until simplex 47, as the difference between the three consecutive error values and DF were below 2×10^{-2}, which was the stopping criterion considered (Figure 2 and Figure 3D). The smallest percentage errors obtained in simplex 47 were 5.35% for NaCl and 4.77% for KCl. These values were considered adequate and similar to those found by Bordin *et al.*[9] and Bona *et al.*[43] when they studied the diffusion of these salts in
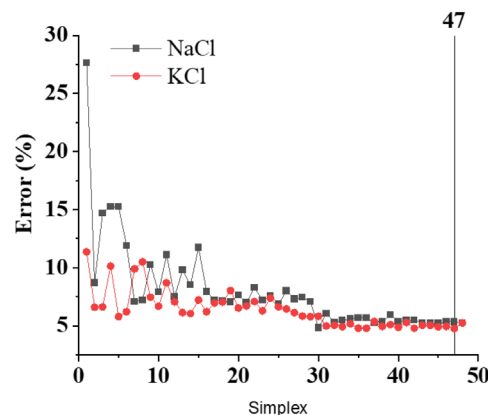

Figure 2. *Convergence of NaCl and KCl percentage error values during simplex optimization*

champignon mushrooms and cheese, respectively. In the present study, errors had their variation minimized from the simplex 45 onwards, as can be seen in Figure 2.

Figure 3 shows the values convergence of the cross coefficients D_{12}, D_{21} (Figure 3A), main coefficients D_{11}, D_{22} (Figure 3B), Biot number (Figure 3C) and the value of the DF desirability function (Figure 3D). This convergence occurred due to joint optimization that provided an adjustment of the error responses simultaneously (Figure 3D).

Table 3 shows the values of the coefficients obtained by simplex optimization. The diffusion of ions in the olive, even verified in the occluded water of the solid matrix, results in effective coefficients much smaller than the diffusion coefficients of the sodium and potassium ions in very dilute aqueous solutions, which are 1.334×10^{-9} m^2 s^{-1} and 1.957×10^{-9} m^2 s^{-1}, at 25 ºC, for NaCl and KCl respectively.[44] This happens due to the interactions of solutes with proteins, carbohydrates, lipids, fibers and inorganic constituents present in the biosolid matrix, in addition to the presence of irregular and tortuous pores within its structure.[18,45]

Depending on the chemical composition of the food, the main diffusion coefficients may differ when compared to each other. According to Borsato *et al.*,[33] quail egg cooked with 74% moisture, which is characterized as a solid protein matrix, when subjected to immersion in brine with 3% salt (70% NaCl: 30% KCl), presented main diffusion coefficients of 8.047×10^{-10} m^2 s^{-1} and 1.185×10^{-10} m^2 s^{-1} for NaCl and KCl, respectively. Bordin *et al.*[9] studying the salting process in champignon mushrooms, determined main diffusion coefficients of 0.2692×10^{-9} m^2 s^{-1} and 0.2953×10^{-9} m^2 s^{-1} for NaCl and KCl respectively.

In a high-fat food, Oliveira *et al.*[46] showed that in Prato cheese with 39.00% moisture, immersed in brine containing 70% NaCl: 30% KCl, the main diffusion coefficients were 0.5×10^{-9} m^2 s^{-1} and 0.3×10^{-9} m^2 s^{-1} for NaCl and KCl, respectively, and Clemente *et al.*[11]

found main diffusion coefficients of 1.12×10^{-9} m^2 s^{-1} and 0.91×10^{-9} m^2 s^{-1} for NaCl and KCl in the salting process of mozzarella cheese with 45.68% moisture.

In the present work, as the olive used (Table 1) presented high moisture content and low protein and lipid content, the main diffusion coefficient of potassium chloride was 1.24 times greater than the sodium chloride, not suffering great influence of these olive constituents, a behavior similar to that verified by Bordin *et al.*[9]

The value of the potassium cross-coefficient is 1.12 times greater than the sodium, which suggests that the potassium flow interferes more with the sodium flow than this the potassium flow. Also, the cross coefficients are much smaller than the main ones, which is expected, since the diffusion to the gradient itself is more important than the interference of one solute in the flow of the other.[33,47]

The film coefficient (h_m) value of potassium chloride (1.2499×10^{-8} m s^{-1}) is greater than the sodium chloride (1.0072×10^{-8} m s^{-1}) indicating that the diffusion of sodium chloride suffers greater influence on the film formed on the surface during the salting process.

The Biot number optimized in the diffusion process was 82.05, indicating that there is an interference from a film formed on the contours of the olive surface. According to Borsato *et al.*,[33] the lower the Biot number, the greater the influence of the layer on the flow of inorganic components at the interface, thus limiting the diffusion by external resistance. The increase in the Biot number indicates less influence of the barrier on mass transfer, with dominant internal resistance. According to Bona *et al.*,[43] the external resistance can be considered negligible when the Biot number is equal to or greater than 200.

Figure 4 shows the distribution profile of sodium and potassium chloride during the olive salting process. The dots represent the experimental data and the lines the data simulated by the finite element method.
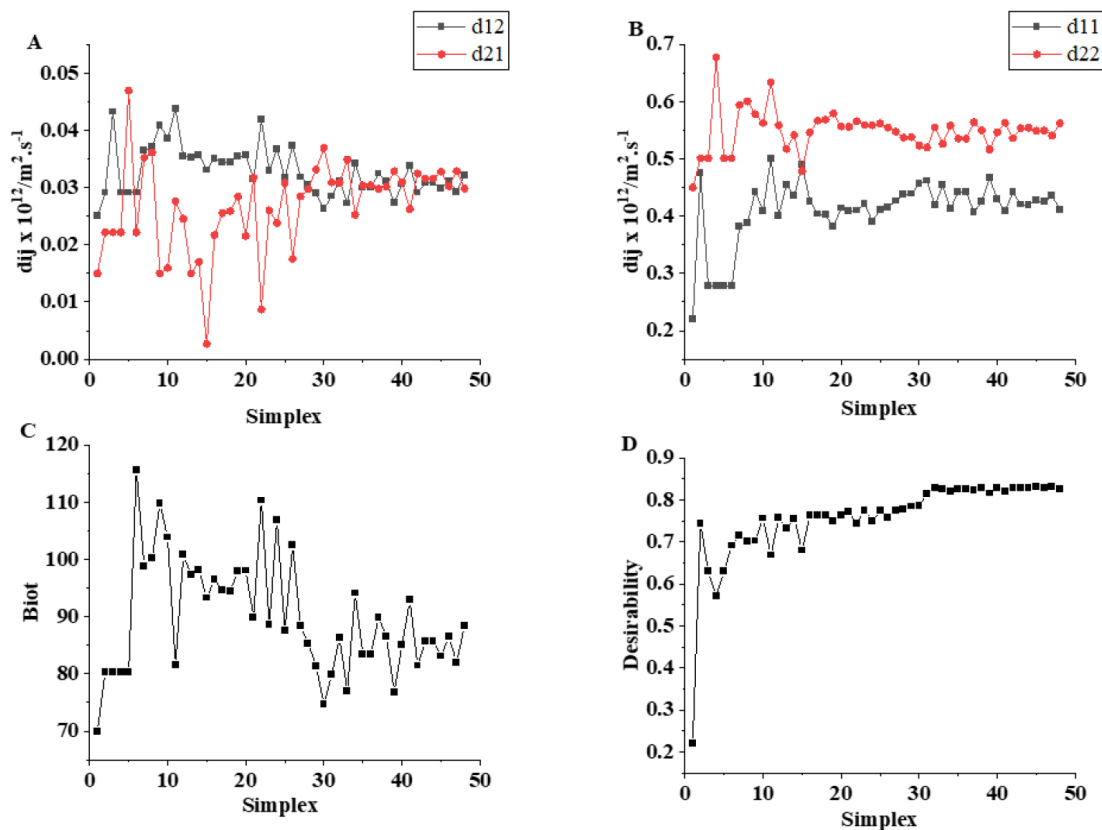

Figure 3. *Variation of the main coefficients D_{11}, D_{22}, cross D_{12}, D_{21}, Biot and DF (desirability function) during the simplex optimization*

Table 3. Main and cross-diffusion coefficients, Biot number, mass transfer coefficient and the percentage error of the diffusion experiment

	NaCl	KCl
Main diffusion coefficient ($m^2 s^{-1}$)	0.4358×10^{-12} (D_{11})	0.5408×10^{-12} (D_{22})
Cross diffusion coefficient ($m^2 s^{-1}$)	0.0293×10^{-12} (D_{12})	0.0329×10^{-12} (D_{21})
h_m (m s^{-1})	1.0072×10^{-8}	1.2499×10^{-8}
Error (%)	5.35	4.77
h_m/λ_m (m^{-1})	23,112.1127	
Biot	82.05	

Biot number estimated to the *x*-axis. (h_m): mass transfer coefficient. (λ_m): diffusivity coefficient.

We can see in Figure 4 that the diffusion of salts is not linear, as there is a greater increase in the concentration in the first hours of salting and that the concentration of salts, obtained by simulation, shows a tendency to increase even after 60 hours of salting.
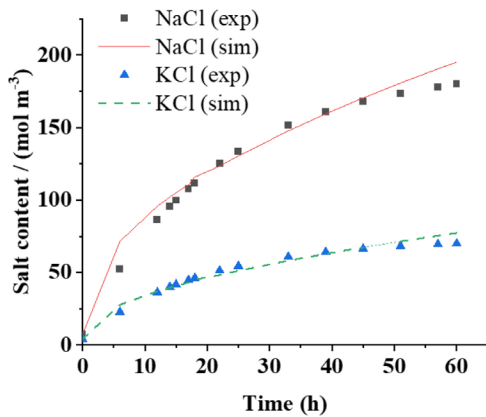

Figure 4. NaCl and KCl distribution profile during salting. The experimental data for NaCl are represented by (■) and KCl (▲), and the simulated data by (—) for NaCl and (···) for KCl

Figure 5 shows the salts distribution profile by simulation, along the X axis, during 333 days for NaCl and 208 days for KCl, the necessary time for the salts' concentration in the olive pulp to be similar to the brine concentration.
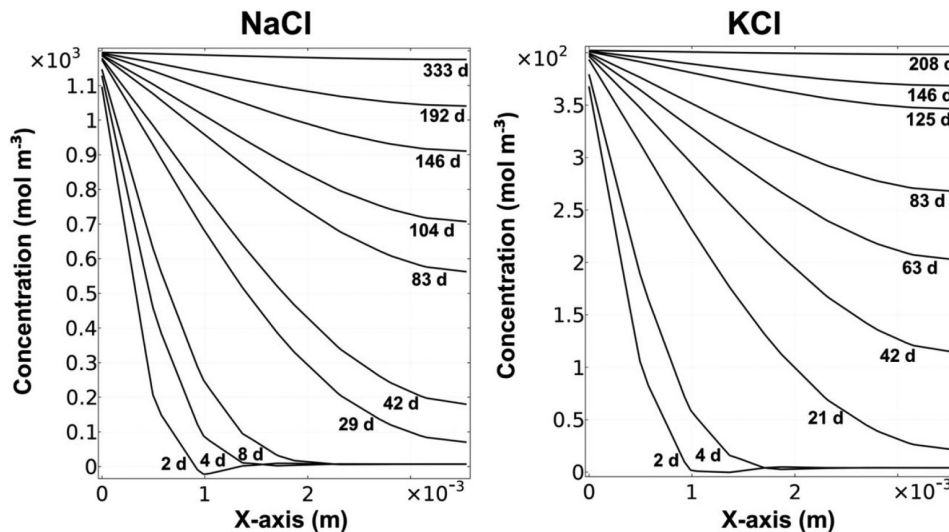
The shorter time for KCl reach equilibrium is because it has a higher principal diffusion coefficient when compared to NaCl, despite having a lower concentration in the brine. It is possible to observe in Figure 5 that the concentrations on the surface of the biosolid (x = 0), in the initial times, are not the same as the boundary conditions represented by the concentration of NaCl and KCl in the used brine. This happens due to the influence of a resistive film on the surface, verified by the dimensionless mass Biot number determined, 82.05. However, with increasing salting time, above 83 days for NaCl and 42 days for KCl, the concentrations converge to the values of the salt concentration in the brine, assuming the Dirichlet boundary condition.[48] The different times observed indicate that the resistive influence of the film is not the same for the diffusion of NaCl and KCl.

Figure 6 shows the distribution of simulated concentrations, in biosolid slices, during the salt diffusion process up to 333 days for NaCl and 208 days for KCl.

According to Figure 6, after 8 and 4 days of diffusion for NaCl and KCl, respectively, 25% of the salts had already been incorporated by the olive pulp, 29 and 21 days, 50% and 83 and 63 days 75%. This indicates that the diffusion is not linear, being faster in the first days of salting. On 192 and 125 days, 95% and equilibrium are reached after 333 days for NaCl and 208 days for KCl.

CONCLUSION

The optimization of the main, crossed and h_m/λ_m coefficients were performed associating the simplex optimization with the desirability functions and the finite element method (FEM). This model associated with simplex optimization proved to be a good tool in simulating the diffusion of the salt during the olive salting process, predicting the final concentration of solutes at a given time.

The amount of salt transferred to the interior of the food did not show a linear relationship with the salting time, since the highest concentrations of salts were observed in the first days of the process.

The presence of a resistive layer on the surface of the olive was verified, causing interference in the salts' diffusion, confirmed by the mass Biot number obtained.

The mathematical modeling of the diffusion process during the olives salting, through the finite element formulation, served to predict the final concentration of solutes as well as at a given time and/or position.

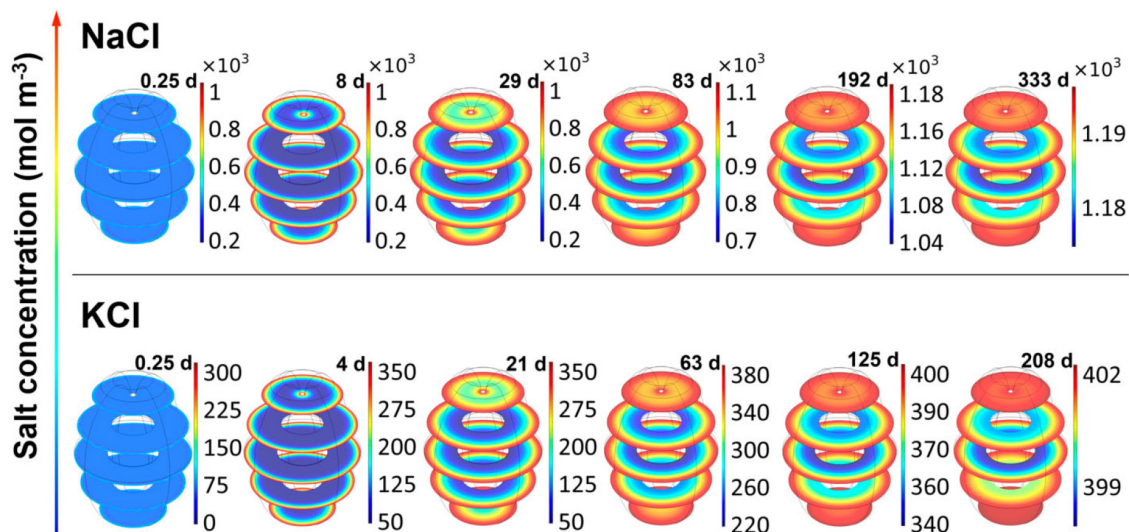The study of the diffusion of the salt in foods has gained

Figure 5. Salt distribution profile during the simulation of the salting process during 333 hours for NaCl and 208 hours for KCl

Figure 6. *Distribution of NaCl and KCl concentrations (mol m⁻³) in the olive sample during the diffusion process after 333 days and 208 days respectively*

prominence due to the interest of consumers who are looking for foods with lower sodium content. In addition, the concentration of salt and its distribution within the food are relevant parameters responsible for the quality and acceptance of the final product.

REFERENCES

1. Brenes, M.; Rejano, L.; Garcia, P.; Sanchez, A. H.; Garrido, A.; *J. Agric. Food Chem.* **1995**, *43*, 2702. [Crossref]
2. Kiritsakis, A. K.; *J. Am. Oil Chem. Soc.* **1998**, *75*, 673. [Crossref]
3. Nergiz, C.; Engez, Y.; *Food Chem.* **2000**, *69*, 55. [Crossref]
4. Colak, N.; Hepbasli, A.; *J. Food Eng.* **2007**, *80*, 1188. [Crossref]
5. Rejano, L.; Montaño, A.; Casado, F. J.; Sánchez, A. H.; de Castro, A.; In *Olives and Olive Oil in Health and Disease Prevention*, 1st ed.; Academic Presss: London, 2010.
6. Aydar, A. Y.; *Food Sci. Technol.* **2021**, *41*, 238. [Crossref]
7. Marsilio, V.; Campestre, C.; Lanza, B.; De Angelis, M.; Russi, F.; *Acta Hortic.* **2002**, *586*, 617. [Crossref]
8. Panagou, E. Z.; Hondrodimou, O.; Mallouchos, A.; Nychas, G.-J. E.; *Food Microbiol.* **2011**, *28*, 1301. [Crossref]
9. Bordin, M. S. P.; Borsato, D.; Cremasco, H.; Galvan, D.; Silva, L. R. C.; Romagnoli, É. S.; Angilelli, K. G.; *Food Chem.* **2019**, *273*, 99. [Crossref]
10. Bautista-Gallego, J.; Arroyo-López, F. N.; López-López, A.; Garrido-Fernández, A.; *LWT--Food Sci. Technol.* **2011**, *44*, 120. [Crossref]
11. Clemente, M. A. J.; de Oliveira, T. F.; Cremasco, H.; Galvan, D.; Bordin, M. S. P.; Moreira, I.; Borsato, D.; *Heat Mass Transfer* **2020**, *56*, 2203. [Crossref]
12. Corsetti, A.; Perpetuini, G.; Schirone, M.; Tofalo, R.; Suzzi, G.; *Frontiers in Microbiology* **2012**, *3*, 1. [Crossref]
13. Lanza, B.; In *Olive Germplasm - The Olive Cultivation, Table Olive and Olive Oil Industry in Italy*; Muzzalupo, I., eds.; Intechopen: London, 2012.
14. Crank, J.; In *The Mathematics of Diffusion*, 2nd ed.; Oxford University Press: London, 1975.

15. Cevoli, C.; Panarese, V.; Catalogne, C.; Fabbri, A.; *J. Food Eng.* **2020**, *270*, 109769. [Crossref]
16. Fadiji, T.; Ashtiani, S. H. M.; Onwude, D. I.; Li, Z.; Opara, U. L.; *Foods* **2021**, *10*, 869. [Crossref]
17. Schwartzberg, H. G.; Chao, R. Y.; *Food Tech.* **1982**, *36*, 73. [Crossref] acessado em 13/12/2022
18. Cremasco, H.; Galvan, D.; Angilelli, K. G.; Borsato, D.; de Oliveira, A. G.; *Food Sci. Technol.* **2019**, *39*, 173. [Crossref]
19. Rakotondramasy-Rabesiaka, L.; Havet, J. L.; Porte, C.; Fauduet, H.; *Sep. Purif. Technol.* **2010**, *76*, 126. [Crossref]
20. Puri, V. M.; Anantheswaran, R. C.; *J. Food Eng.* **1993**, *19*, 247. [Crossref]
21. Wang, L.; Sun, D. W.; *J. Food Eng.* **2002**, *51*, 319. [Crossref]
22. Shokouhmand, H.; Abadi, S. M. A. N. R.; *Heat Mass Transfer* **2010**, *46*, 891. [Crossref]
23. Cekmecelioglu, D.; Uncu, O. N.; *Food & Nutrition Journal* **2016**, *1*, 1. [Crossref]
24. Chung, T. J.; In *Finite element analysis in fluid dynamics - NASA STI/ Recon Technical Report A*, nº 78, McGraw Hill: New York, 1978.
25. Zienkiewicz, O. C.; Morgan, K.; In *Finite Elements and Aproximation*, 1st ed.; John Wiley & Sons Ltd: New York, 1983, cap. 7.
26. Spendley, W.; Hext, G. R.; Himsworth, F. R.; *Technometrics* **1962**, *4*, 441. [Crossref]
27. Onsager, L.; *Annals of the New York Academy of Sciences* **1945**, *46*, 241. [Crossref]
28. Bona, E.; da Silva, R. S. S. F.; Borsato, D.; Silva, L. H. M.; Fidelis, D. A. S.; *J. Food Eng.* **2007**, *79*, 771.[Crossref]
29. Angilelli, K. G.; Orives, J. R.; da Silva, H. C.; Coppo, R. L.; Moreira, I.; Borsato, D.; *J. Food Process. Preserv.* **2015**, *39*, 329. [Crossref]
30. Harrington, E. C.; *Industrial quality control* **1965**, *21*, 494. [Crossref] acessado em 13/12/2022
31. Derringer, G.; Suich, R.; *Journal of Quality. Technology* **1980**, *12*, 214. [Crossref]
32. *Comsol Multiphysics®, version 5.2*; COMSOL Inc., Burlington, MA, USA, 2016.
33. Borsato, D.; Moreira, M. B.; Moreira, I.; Pina, M. V. R.; Silva, R. S. S. F.; Bona, E.; *Food Sci. Technol.* **2012**, *32*, 281. [Crossref]
34. Öngen, G.; Sargin, S.; Tetik, D.; Köse, T.; *Food Technol. Biotechnol.* **2005**, *43*, 181. [Crossref]
35. Malheiro, R.; Casal, S.; Sousa, A.; de Pinho, P. G.; Peres, A. M.; Dias, L. G.; Bento, A.; Pereira, J. A.; *Food Bioprocess Technol.* **2012**, *5*, 1733. [Crossref]

36. da Saúde, C. E. V. C.; Dissertação de Mestrado, Universidade do Algarve, Portugal, 2014. [Crossref]

37. Ünal, K.; Nergiz, C.; *Grasas y Aceites* **2003**, *54*, 71. [Crossref]

38. Fernándes, A. G.; Fernández-Diez, M. J. In *Table Olives:Production and Processing*, 1997th ed.; Chapman & Hall: London, 1997.

39. Gómes, A. H. S.; García, P. G.; Navarro, L. R.; *Grasas y Aceites* **2006**, *5*, 86. [Crossref]

40. Hurtado, A.; Reguant, C.; Esteve-Zarzoso, B.; Bordons, A.; Rozès, N.; *Food Res. Int.* **2008**, *41*, 738. [Crossref]

41. Cardoso, S. M.; Mafra, I.; Reis, A.; Nunes, C.; Saraiva, J. A.; Coimbra, M. A.; *LWT--Food Sci. Technol.* **2010**, *43*, 153. [Crossref]

42. Angelis, P. N.; Mendonça, J. C.; da Rocha, L. R.; Capelari, T. B.; Prete, M. C.; Segatelli, M. G.; Borsato, D.; Tarley, C. R. T.; *Electroanalysis* **2020**, *32*, 1198. [Crossref]

43. Bona, E.; da Silva, R. S. S. F.; Borsato, D.; Silva, L. H. M.; Fidelis, D. A. S.; *Cienc. Tecnol. Aliment. (Campinas, Braz.)* **2010**, *30*, 955. [Crossref]

44. Lide, D. R.; Frederikse, H. P. R. In *Handbook of Chemistry and Physics*, 78th ed., CRC-Press: Boca Raton, 1997.

45. Geurts, T. J.; Walstra, P.; Mulder, H.; *Neth. Milk Dairy J.* **1974**, *28*, 102. [Crossref] acessado em 06/12/2022.

46. Oliveira, T. F.; Clemente, M. A. J.; Galvan, D.; Fix, G.; Mantovani, A. C. G.; Borsato, D.; *Cienc. Tecnol. Aliment. (Campinas, Braz.)* **2020**, *40*, 482. [Crossref]

47. Borsato, D.; Moreira, I.; Nóbrega, M. M.; Moreira, M. B.; da Silva, R. S. S. F.; Bona, E.; *Quim. Nova* **2009**, *32*, 2109. [Crossref]

48. Bona, E.; Carneiro, R. L.; Borsato, D.; da Silva, R. S. S. F.; Fidelis, D. A. S.; Silva, L. H. M.; *Braz. J. Chem. Eng.* **2007**, *24*, 337. [Crossref]